Cell Tissue Res (2006) 325: 361–368
DOI 10.1007/s00441-006-0182-8

REGULAR ARTICLE

Michal Raz-Bahat · Jonathan Erez · Baruch Rinkevich

In vivo light-microscopic documentation for primary calcification processes in the hermatypic coral *Stylophora pistillata*

Received: 21 September 2005 / Accepted: 1 February 2006 / Published online: 28 March 2006

Abstract Skeletogenesis in the hermatypic coral *Stylophora pistillata* was studied by using the lateral skeleton preparative (LSP) assay, viz., a coral nubbin attached to a glass coverslip glued to the bottom of a Petri dish. Observations on tissue and skeletal growth were made by polarized microscopy and by using vital staining. The horizontal distal tissue edges developed thin transparent extensions of ectodermal and calicoblastic layers only. Four stages (I-IV) of skeletogenesis were observed at these edges, underneath the newly developed tissue. In stage I, a thin clear layer of coral tissue advanced 3–40 μm beyond the existing LSP peripheral zone, revealing no sign of spiculae deposition. At stage II, primary fusiform crystals (1 μm each) were deposited, forming a primary discontinuous skeletal front 5–30 μm away from the previously deposited skeleton. During stage III, needle-like crystals appeared, covering the primary fusiform crystals. Stage IV involved further lengthening of the needle-like crystals, a process that resulted in occlusion of the spaces between adjacent crystals. Calcification stages I-III developed within hours, whereas stage IV was completed in several days to weeks. Two basic skeletal structures, "scattered" and "laminar" skeletons, were formed, integrating the growth patterns of the needle-like crystals. High variation was recorded in the expression of the four calcification stages, either between different locations along a single LSP or between different preparations observed at the same diurnal time. All four skeletogenesis stages took place during both day and night periods, indicating that an intrinsic process controls *S. pistillata* calcification.

Keywords Biomineralization · Calcification · Nubbin · Polarized-light microscopy · *Stylophora pistillata* (Cnidaria)

This study was supported by the Israel Science Foundation (206/01 to J.E.), by the BARD, US-Israel Bi-National Agricultural Research and Development, by INCO-DEV project (REEFRES), and by CORALZOO, EC Collective Research project.

M. Raz-Bahat · B. Rinkevich (✉)
Israel Oceanographic and Limnological Research,
National Institute of Oceanography,
P.O. Box 8030, Haifa 31080, Israel
e-mail: buki@ocean.org.il
Tel.: +972-4-8565275
Fax: +972-4-8511911

M. Raz-Bahat · J. Erez
Institute of Earth Sciences, The Hebrew University,
Jerusalem 91904, Israel

Introduction

Microstructures of $CaCO_3$ skeletons have been studied in detail in a number of scleractinian corals. Light-microscopic studies have revealed the existence of three-dimensional fan-like systems of crystals radiating from centers of calcification foci (Ogilvie 1896; Barnes 1970) that cumulatively create larger structures termed fasciculi (Wise 1972) and trabeculae (see Barnes 1970). With the help of electron-microscopic methods, primary crystals (up to 19 nm), which are the basic skeletal elements of the above structures, have been detected (Gladfelter 1982, 1983; Constantz 1986, 1989; Isa 1986; Le Tissier 1988; Hidaka 1991; Hidaka and Shirasaka 1992; Clode and Marshall 2003a).

At the same time, studies have also been carried out on coral tissue structures (Johnston 1980; Wright and Marshall 1991; Marshall and Wright 1993), detailing coral tissue layers and their cells. Special attention has been paid to the calicoblastic layer, which is in contact with the coral skeleton. Moreover, the presence of organic macromolecules has been revealed between the calicoblastic layer and the skeleton; these molecules create the organic matrix for coral skeletons (Wainwright 1963; Young 1971, 1973; Johnston 1980; Marin et al. 1996; Allemand et al. 1998; Cuif et al. 1999; Clode and Marshall 2003b; Cuif and Dauphin 2005). Since most scleractinian corals possess symbiotic photosynthetic algae (for a review, see Muscatine 1990), their roles have been evaluated in coral calcification. Pioneering investigations by Goreau (1959) and Barnes (1970) have laid the foundation for the prevailing dogma that light enhances calcification in hermatypic corals. This

tenet has been ratified by follow-up studies (Johnston 1980; Gladfelter 1982, 1983; Le Tissier 1988; Gattuso et al. 1999; Furla et al. 2000) but has been challenged by others (Rinkevich and Loya 1984).

Calcification in hermatypic corals is a biological phenomenon characterized by complex activities. For example, studies on coral species have revealed that different types of crystals are deposited at various sites, in concert with the diurnal cycle (Barnes 1972; Gladfelter 1982, 1983; Le Tissier 1988; Howe and Marshall 2002), whereas in other species, this diurnal pattern does not exist (Hidaka 1991; Clode and Marshall 2003b). The calicoblastic tissue has been shown to react harmoniously with the calcification processes by developing numerous underlying pockets (Gladfelter 1983; Le Tissier 1990), by lifting behavior (Barnes 1972; Isa 1986), or by tissue thickening (Le Tissier 1988).

Here, we have monitored, for the first time in vivo, the micro-structural details of crystal accretion in a branching coral form. We have employed the lateral skeleton preparative (LSP) assay (Reynaud-Vaganay et al. 1999; Shafir et al. 2001, 2003) in which observations are made on flat transparent coral tissue growing on coverslips. Any small calcium carbonate crystals (>1 μm) deposited can be easily scrutinized under the microscope. Moreover, skeletal and tissue elements can be more readily distinguished by using a polarization device. The LSP assay has allowed us to follow-up sequences of events that are associated with coral calcification and has provided us with opportunities to clarify questions related to the structure of the calicoblastic tissue and the association between diurnal cycles and calcification events in *Stylophora pistillata*.

Materials and methods

Collection and cultivation of corals

Stylophora pistillata branches were collected from a shallow flat reef, at 1–4.5 m depth, in front of the Inter-University Institute for Marine Science in Eilat, Israel, and placed into an outdoor flowing seawater tank system. They were dissected with a cutter into fragments (nubbins) that were 0.5–3 cm in size. Each nubbin was glued (by Super Glue (Loctite, UK) or by underwater epoxy glue (Aqua Mend, USA) to a thin coverslip, pre-glued (Elastomer Kit, Belgar, UK) to a window on the bottom of a 5-cm plastic Petri dish (Fig. 1a). LPS dishes were transferred to an

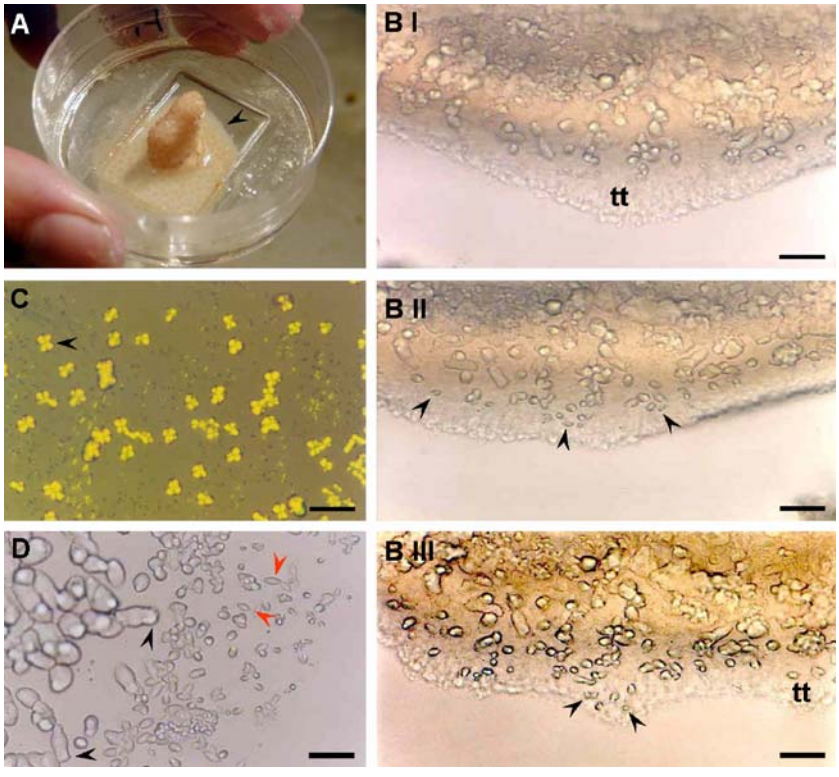

Fig. 1 **a** Lateral skeleton preparative (LSP) assay. A small branch of *S. pistillata* glued onto a microscope coverslip. A thin disk of coral tissue and skeleton of about 3.5 cm diameter (*black arrowhead*) is formed on the substrate, 5 weeks thereafter. **b** Sequence of skeletogenesis events in *S. pistillata* LSP assay; phase contrast. ×600. **bi** Skeletogenesis stage I; new marginal tissue expansion (*tt*) devoid of symbionts and deposited skeletal crystals. **bii** Skeletogenesis stage II, 1 h later. Small primary crystals (*black arrowheads*) first appear under the rim of the expanded tissue. **biii** Development of an additional cycle of tissue expansion (*tt*) and a new set of primary crystals (*black arrowheads*), 1 h later. **c** *S. pistillata* colony. Half-polarized light microscopy. Crystal bundles present dark and glowing areas according to crystal orientation and resemble a shaded cross (*black arrowheads*); this appears when all crystals are set perpendicular to the center. ×600. **d** Skeletogenesis stage III. Exposed (without tissue) marginal area in the LSP assay. Localization of secondary needle-like crystals (*black arrowheads*) and primary fusiform crystals (*red arrowheads*). ×600. *Bar* 10 μm (for **b-d**)

indoor flowing seawater system at the National Institute of Oceanography, Haifa, Israel, where they were maintained in a wide water table (24°C) lit by artificial illumination (Metal Halide cool white, 150 W, Philips IP65; 12:12 L:D).

In vivo observations

We used an inverted microscope (Zeiss, Reichert) equipped with polarization equipment. Time-lapse observations were performed on peripheral zones of the LSP assay. These observations were made on developing tissues at diamond-penned pre-marked sites or on unmarked sites at designated hours of the day. The dishes (each containing 50 ml seawater) were arranged on the microscope stage such that the thin lateral tissues developing on the glass substrates could be observed (at magnifications of ×400 to ×1,000) and photographed by a still camera (Nikon M-35) or a video camera (Supercam, Applitec, Israel).

Histological observations

Histological observations were performed on the newly expanded, flat, coral tissues. Nubbins were anesthetized by Quinaldine solution for 30 min and fixed in Bouin's solution for 2 h. Previously marked sites of interest were gently cut and peeled off the glass substrate by surgical blades. The tissue samples were dehydrated in increasing concentrations of ethanol, transferred to a graded series of buthanol/ethanol mix, and embedded in paraffin. Serial cross and longitudinal sections (4–5 μm) were cut on a microtome and stained with Alum/Erhlich hematoxylin and eosin.

In-situ skeletal labeling with tetracycline

We used tetracycline solution (tetracycline-hydrochloride $C_{22}H_{24}N_2O_5$.HCl; Sigma), a non-toxic antibiotic, in various applied concentrations (Rowley and Mackinnon 1995) to achieve binding to newly deposited calcium carbonate crystals during incubation. Excitation at a wavelength of 360 nm caused the emission of a typical 560-nm

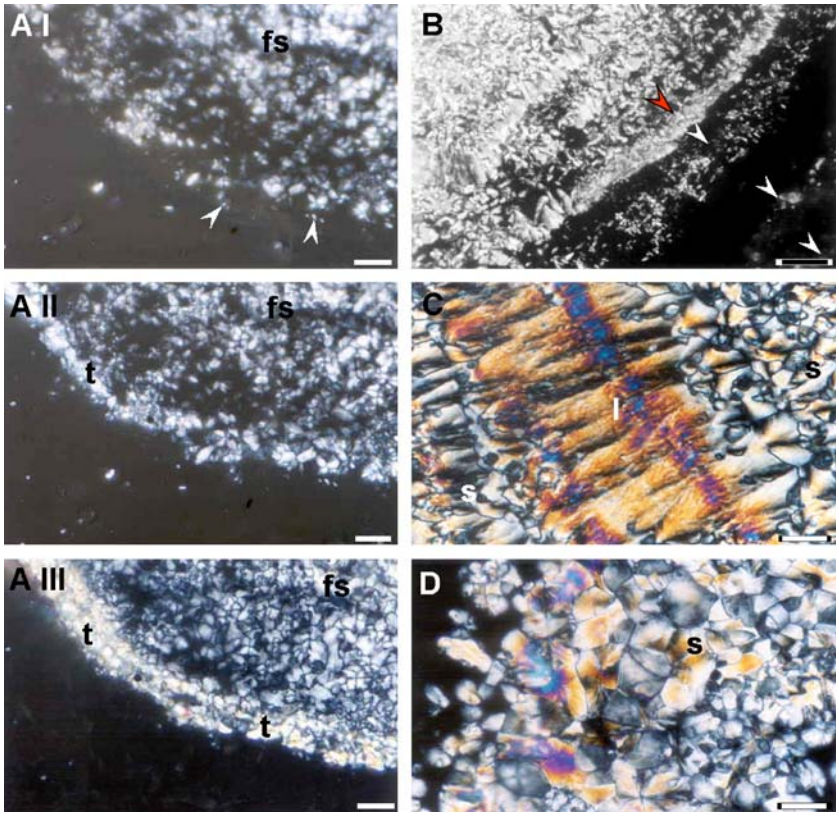

Fig. 2 **a** Calcification processes in *S. pistillata* LSP assay; polarized light. ×400. **ai** Skeletogenesis stage II. Primary fusiform crystals (*white arrowheads*) are deposited randomly at the front edge of the coral tissue, approximately 10 μm from the former skeleton (*fs*). **aii** Skeletogenesis stage IV. Simultaneous consecutive needle deposition result in skeletal "terraces" (*t*) that are formed parallel to the former skeleton (*fs*). **aiii** A developed terrace structure (*t*) formed by continuous elongation and thickening of the needle-like crystals. *Bar* 20 μm (for *ai-aiii*). **b** Skeletogenesis stage IV (*red arrowhead*) can be compared with late stages at distal areas (*white arrowheads*) that include skeletogenesis stages I-III elements; polarized light. ×400. *Bar* 20 μm. **c, d** Higher magnification of skeletogenesis stage IV; polarized light. Crystal deposition results in two skeletal structures: a laminar pattern (*l*) constructed of three-dimensional fans that form colorful laminar lines under polarized light and a scattered (*s*) pattern that develops when shorter needles radiate randomly outward. ×1,000. *Bar* 5 μm

yellow-green light. Tetracycline (1% stock solution) was stored at −20°C in the dark (foil paper) to prevent light reactions. Incubations were performed for 2 h to mark crystals deposited at the beginning of the observation time, and dishes were then washed with fresh seawater. Photographs were taken to evaluate skeletogenesis and calcification stages during the daytime (6:00–18:00) or nighttime (18:00–6:00). This protocol of employing only two photographic sessions per 24 h minimized the possible impacts from the light of the microscope during photography and yet provided us with images of diurnal events.

Results

Four initial stages of skeletogenesis

As recorded previously (Reynaud-Vaganay et al. 1999; Shafir et al. 2001, 2003), lateral tissue extension, which firmly attached the nubbin to the substrate, developed within 3 weeks after LSP initiation. This was followed by rapid extension of transparent coral tissue (initially devoid of zooxanthellae), which, at advanced stages, formed a thin disk of skeleton and tissue of about 3–4 cm in diameter (nubbin diameter: ~1 cm) on the substrate.

Time-lapse-microscopic observations on marked sites along LSP margins and detailed observations at peripheral sites sporadically chosen at various times of the day revealed a pattern of calcification characterized by four distinct skeletogenesis stages (I-IV). Stage I was the phase of expanded new marginal tissue (Fig. 1bi) forming a thin transparent double-decked epithelial tissue on the substrate, devoid of symbionts and calcium carbonate crystals. Secretion of primary fusiform needles (crystals) underneath the edge of this thin expanded coral tissue (Fig. 1bii, biii) was characteristic of skeletogenesis stage II. The primary crystals were 1 μm in diameter, at first, but then grew to 3 μm. Crystals were deposited at a distance of up to 30 μm from the older marginal skeleton and were arranged randomly. Each primary crystal was a solitary crystal (not a bundle of crystals), since it uniformly transmitted polarized light and darkened uniformly when polarization was removed. Crystal bundles, on the contrary, were typically dark with glowing areas under polarized light at various crystal orientations (Fig. 1c).

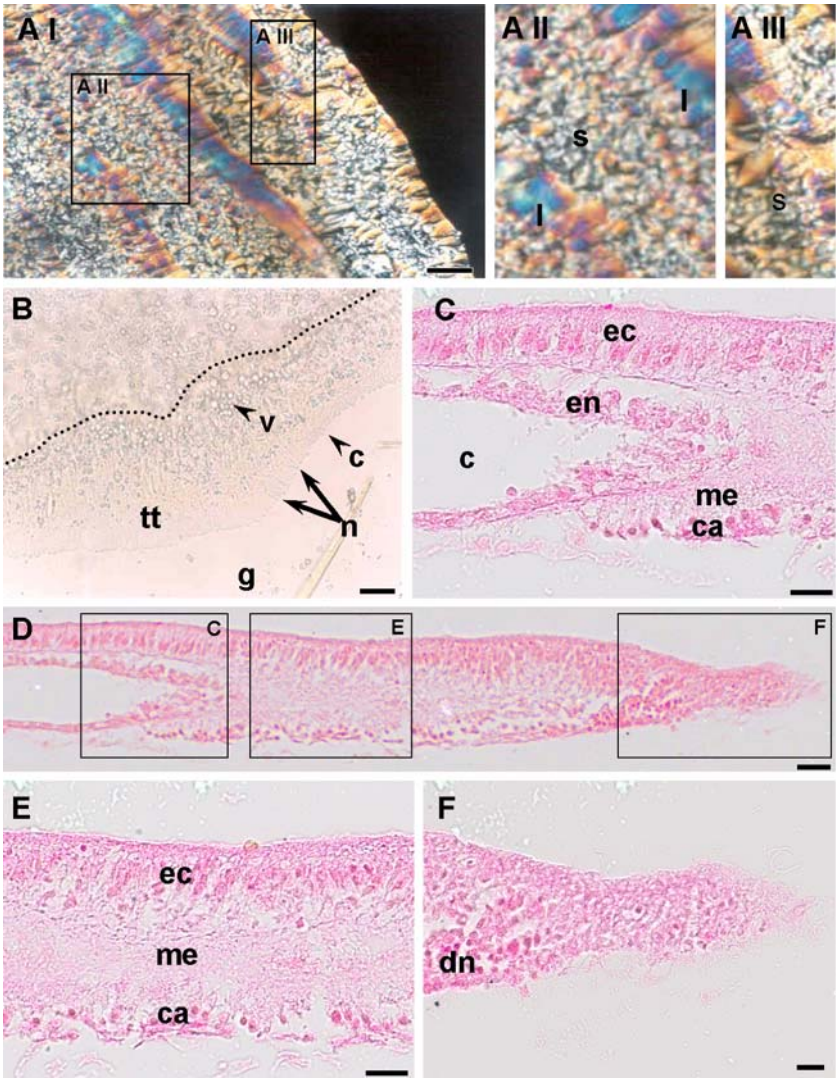

Fig. 3 **ai** End of skeletogenesis stage IV; polarized light. **aii**, **aiii** Laminar (*l*) or scattered (*s*) calcification patterns develop, respectively, either consecutively or simultaneously at different sites along the LSP margins. ×100. *Bar* 40 μm. **b** LSP edge; phase contrast. Transparent expanded marginal tissue (*tt*) on the glass substrate (*g*) is devoid of symbiotic algae and skeletal crystals but possesses nematocysts (*n*) and cytoplasmic projections (*c*). A clear border (*dashed line*) demarcates the regular and proximal edges of the expanding tissue (*tt*), with small goups of vacuoles (*v*). ×400. *Bar* 20 μm. **c-f** Expanded marginal LSP tissue (longitudinal section, hematoxylin and eosin staining; **c**, **e**, **f** enlarged areas of **d**). The upper ectodermal layer (*ec*) is composed of elongated cells, with light acidophilic cytoplasm. The calicoblastic cells (*ca*) each have a round dark nucleus. In **c** (proximal to the nubbin), two layers of endodermis (*en*) can be observed separated by the gastrovascular cavity (*c*). In **e**, the calicoblastic layer (*ca*) and upper ectodermis (*ec*) coalesce, with a mesoglea (*me*) in between. In **f**, disorganized aggregations of cells with distinct nuclei (*dn*) are observed at the area where both ectodermal layers join. ×1,000. *Bar* 10 μm (**c**, **e**, **f**). ×200. *Bar* 20 μm (**d**)

At skeletogenesis stage III, secondary needle-like crystals were deposited on top of the primary fusiform crystals, creating a crystal cluster (Fig. 1d). At first, these secondary crystals appeared and elongated at the two poles of the fusiform primary crystal; subsequently, they grew in all directions. The continuous calcification process by secondary needles and the extension of existing needle-like crystals resulted in the occlusion of the small spaces between the crystals. Because of consecutive "waves" during calcification stage III, a typical skeletal "terrace" structure was formed peripherally, parallel to the former skeletal ridge (Fig. 2a,b). Skeletogenesis stage IV was determined as the major space-filling phase, performed by calcium needle elongation and calcium carbonate deposition between the skeletal terraces. Macroscopically, at the end of this stage, an even sheet of calcium carbonate was formed on the substrate (Figs. 2b-d, 3a). Stages I–III were completed within a few hours, whereas stage IV was a slow process, taking up to a several weeks to occur. We also observed several repeated cycles of stages I–III that were started and completed prior to the onset of stage IV (Fig. 2b).

At the morphological level, the needle-like crystals formed two dissimilar skeletal structures. The first, termed as having a "laminar skeletal pattern" (Fig. 2c), was shaped as laminar lines and was colorful under polarized light. This structure developed during calcification stage IV, when parallel needles radiated in a single direction. The second skeletal structure (Fig. 2d), termed as having a "scattered skeletal pattern", reflected the growth pattern of relatively shorter needles radiating randomly outward. The expanded marginal tissue and the fusiform crystals were more readily visible under the microscope during the formation of the scattered skeletal structure than during the formation of the laminar structures. These two types of calcification patterns developed, either alternately or simultaneously, at different sites along the margins of a single preparation (Figs. 2c, 3a).

Tissue structure

Calcification stages I to III were best observed at the most distal sites of the LSP, where the tissue was thin and devoid of any zooxanthella. This enabled us to investigate the fine details of crystal formation and tissue organization in the transparent preparations. Observations revealed that the tissue margins were moveable, could expand forward within 2 h (maximal documented expansion: 320 μm/24 h), and were sensitive to various types of stresses, such as high irradiation or mechanical stimulation. Response to stress started with fast tissue contractions (up to 21 mm/min; revealing, in many cases, exposed crystals on the substrata) and was followed by repeated slower expansions (up to 0.22 μm/min).

Under the light microscopy, several cellular components of the coral tissue were visible at the LSP tissue margins (Figs. 1b, 3b). These included mucocytes, nematocysts, cytoplasmic projections, and constantly beating cilia at the exterior surface of the coral tissue. Continuous movement of small round particles within the cavity of the coelenteron was also observed. The movements of the particles were not observed at the peripheral areas of expanding tissues, indicating that the peripheral zone lacked gastrovascular cavity, a conclusion that was confirmed by the examination of histological sections (Fig. 3c–f). At the proximal expanded tissue edges (Fig. 3c,d), two parallel sets of ectodermal and endodermal layers, separated by the gastrovascular cavity, were clearly detectable. The upper ectodermal layer was characterized by ciliated tall narrow cells with dark elliptic nuclei. A few mucocytes possessing light acidophilic cytoplasmic content were also found. The lower ectodermal layer (the calicoblastic layer) comprised flattened cells containing small round nuclei. The outermost edge of the marginal tissue (Fig. 3d,f) was of special interest as being a site where the calicoblastic and upper ectodermal layers coalesced. During expansion-retraction movements, both ectodermal epithelial layers at the edge moved together in harmony as a single tissue unit that lacked an endodermis and gastrovascular cavity. Only a thin non-cellular mesoglea separated the two sheets of ectodermal layers (Fig. 3d,e). At the contact point between these two ectodermal layers, a mass of disorganized nuclei was found (Fig. 3d,f), which could not be related to either ectoderm.

Diurnal patterns

Since the calcification process in the LSP assay is a continuous phenomenon, the four skeletogenesis stages were grouped into two major phases for long-term diurnal observations: primary calcification (stages I and II) and secondary calcification (stages III and IV), characterized by light and massive calcium carbonate accretion, respectively. Following the finding that different zones in the same LSP (carried out on 16 different *S. pistillata* nubbins; data not shown) represented unsynchronized calcification stages, ten additional experiments were designed to elucidate further possible diurnal variation of primary and secondary calcification phases between different LSPs (Table 1; experiments 5–10) and of groups of nubbins (n=10–16) in which observations were performed along the entire nubbin peripheral zones (Table 1; experiments 1–4). As within a single preparation, high variation was recorded between different nubbins at all times during the day (significant difference between treatments at the same time-point: P=0.011, α=0.002). Using tetracycline-labeled preparations, we recorded calcification patterns at several locations on each LSP (Table 1; n=7–12), during the night (18:00–6:00) and the day (6:00–18:00; Table 1, experiments 5–10). Observations were performed simultaneously: (1) with polarized light to observe the morphology of skeletal crystals; (2) with 360-nm wavelength excitation to observe tetracycline labeling; and (3) under phase contrast to observe the coral tissue. Each of the preparations monitored during the night (Table 1; experiments 5–7) and day (experiments 8–10; Table 1) showed different, some-

times even contrasting, calcification profiles. Therefore, within a single LSP or between different *S. pistillata* LSPs, there was no clear diurnal calcification pattern.

Our results (Table 1) further revealed that the four skeletogenesis stages were abundant during both night and day observations, and that the distribution of primary or secondary stages showed no consistent trend. We therefore concluded that there was no correlation between primary and secondary calcification phases during day or night hours.

Discussion

As we have demonstrated here, the LPS assay can be used as a tool for studying calcification processes in hermatypic corals. The lateral deposited skeleton of *S. pistillata* nubbins in this assay represents and simplifies skeletogenesis processes occurring at the branch tips and provides a unique opportunity for the in vivo observation of detailed tissue-coral associations during early calcification events. Using the LSP assay, we have found a sequence of four skeletogenesis stages that include the appearance of two kinds of crystals: primary fusiform and secondary needle-like crystals. These two types of skeletal crystals resemble crystal descriptions from dead-skeleton analyses of *Stylophora*, *Acropora*, and *Galaxea* species (Gladfelter 1982, 1983; Isa 1986; Le Tissier 1988; Hidaka 1991; Clode and Marshall 2003b). We have also found that the fusiform crystal in *S. pistillata* is a fundamental primary unit in skeletogenesis and not part of the crystal cluster, as recorded by Clode and Marshall (2003a, 2003b) in *Galaxea fascicularis*, and not part of two spherulitic crystals as found by Isa (1986) in *Acropora hebes*.

The first stage of coral tissue expansion in *S. pistillata* does not involve spicule accretion. It resembles former observations of elevated coral tissue above calcified zones (Barnes 1972; Vago et al. 1997), in which over-saturated interfacial regions (Barnes 1970, 1972; Gladfelter 1983) or extracelluar pockets filled with calcium-associated organic material (Clode and Marshall 2003a) have been suggested as sites for crystal deposition. This stage leads to the next two calcification stages in which two kinds of crystals (primary fusiform and secondary needle-like crystals) develop two different types of skeletal structures. These include the "scattered" skeleton, which is formed by short needle-like crystals with random orientation, and the colored "laminar" skeleton, which is formed by needle-like crystals deposited in one direction only. The formation of the skeletal "terrace" structure parallel to the former skeletal ridge (Fig. 2ai-iii), as described in this work, is new, although it clearly resembles scanning electron microscopic (SEM) observations of the apical tip region of *Galaxea fascicularis* reported by Hidaka (1991).

The occlusion stage, viz., the fourth stage of skeletogenesis, develops through the elongation of the needle-like crystals. During our LSP observations, we have not documented any deposition of organic matter in the expanded marginal tissue, although organic materials might be the precursors for the formation of the primary fusiform crystals (Johnston 1980; Cuif et al. 1999; Clode and Marshall 2003a), and the deposition of organic material might play an important role in the skeletal "terrace" formation in *Stylophora* skeletons. In SEM preparations of several other species, Perrin (2003) has shown that the boundaries between two successive lamellae in the coral skeleton are produced by different thicknesses at the bottom of local organic fibers, indicating the importance of organic matter for their formation.

Another important feature of the LSP assay is the accessibility of the transparent tissue, primarily the distal tissue area, during early calcification events. These microscopic observations have revealed a dynamic front tissue area that has the ability to respond by fast contraction and expansion to various challenges. Based on time-lapse photography series (unpublished data), we conclude that the movement of tissue margins (both contraction and expansions) is driven by muscular activity in the proximal site of the LSP, at the base of the expanding tissue. By using SEM analysis of the terminal polyp calicoblastic tissue in *A. cervicornis* colonies, Gladfelter (1983) has observed numerous pockets and projections in the coral

Table 1 Primary and secondary stages (%) of sites observed in *Stylophora pistillata* during various diurnal periods (*n* nubbins in a specific experiment in which observations were taken along the entire nubbin peripheral zone, *s* number of observed sites in a single nubbin)

Experiment number	Duration of observation (h)	Day time	Number of nubbins/sites	Stages (%)		Primary/ secondary
				Primary (±SD)	Secondary(±SD)	
1	2.5	09:30-12:00	16n	13.4±12.3	86.56±12.3	0.2
2	2.5	15:30-17:00	16n	20.0±20.9	80.0±20.9	0.3
3	2.5	16:30-18:00	16n	38.8±25.7	60.0±25.7	0.6
4	2.5	19:30-21:00	10n	31.5±21.9	68.5±21.9	0.5
5	12	18:00-06:00	12s	58.5	41.5	1.4
6	12	18:00-06:00	8s	100	0	–
7	12	18:00-06:00	10s	0	100	0.0
8	12	06:00-18:00	9s	0	100	0.0
9	12	06:00-18:00	7s	43	57	0.8
10	12	06:00-18:00	8s	100	0	0.2

tissue, corresponding to the deposition of fusiform crystals. These snug spaces are suggested to be the sites where the exchange of ions and soluble organic molecules occurs between the interior and exterior of the calicoblastic cells, for the regulation of deposited mineral structure. Barnes (1970, 1972) has proposed that skeletogenesis develops in closed spaces in an over-saturated solution, formed by the uplifting of the calicoblastic epithelium. Le Tissier (1988) has further reported a thicker calicoblastic tissue in areas of massive calcium carbonate deposition. Despite the similarity in the skeletogenetic role of the tissue, the calcifying tissue of *S. pistillata* LSPs lacks intracellular symbionts, forming a flattened calcification site. Histological sections of the periphery have further revealed the coalescence of the two ectodermal layers, which merge into a single flat layer without a gastrovascular cavity or endodermis. We have not recorded, in the LSP assays, any closed space or extracellular pocket between the tissue and the substrate implying a function of exchange of calcium and carbonate ions for new skeleton formation. The results of the present study further reveal a fixed cascade of events during skeletogenesis in *S. pistillata*, including the timing and order of crystal appearance, crystal distribution in space ("terraces" corresponding to the extension pattern of the tissue), and skeletal structures (the scattered skeleton follows tissue extension; the laminar skeleton when no tissue extension occur). This is in agreement with the idea (Johnston 1980; Gladfelter 1982, 1983; Simkiss and Wilbur 1989; Le Tissier 1991; Al-Horani et al. 2003; Clode and Marshall 2003a) that calicoblastic tissue is important in the control of coral calcification.

Our observations made on *S. pistillata* LSP assays, while confirming the conclusion of Hidaka (1991) and Clode and Marshall (2003b) studies, do not support the idea of diurnal changes in calcification patterns and rates (sensu Barnes 1972; Le Tissier 1988; Furla et al. 2000). They are also different from Gladfelter's results (1983) on *A. cervicornis* showing that different types of crystals are deposited during specific diurnal periods. In *Acropora*, fusiform crystals appear with a random orientation, mostly at nighttime and primarily at the elongated spines of the coral septa. Our results, however, strengthen the tenet that an intrinsic fundamental process controls skeletogenesis, even in zooxanthellate corals. Although this conclusion is insufficient to contradict the proposal for ubiquitous "light-enhanced calcification" in hermatypic corals (Goreau 1959; Pearse and Muscatine 1971; Chalker and Taylor 1975; Gattuso et al. 1999), it suggests that, in *S. pistillata* (Rinkevich and Loya 1984) and probably other coral species, several mechanisms might control the calcification processes.

Acknowledgement We thank Dr. E. Moisseva for her help with histological sections.

References

Allemand D, Furla P, Bénazet-Tambutté S (1998) Mechanisms of carbon acquisition for endosymbiont photosynthesis in Anthozoa. Can J Bot 76:925–941

Al-Horani FA, Al-Moghrabi SM, Beer D de (2003) Microsensor study of photosynthesis and calcification in the scleractinian coral, *Galaxea fascicularis*: active internal carbon cycle. J Exp Mar Biol Ecol 288:1–15

Barnes DJ (1970) Coral skeletons: an explanation of their growth and structure. Science 170:1305–1308

Barnes DJ (1972) The structure and function of growth ridges in scleractinian coral skeletons. Proc R Soc Lond (Biol) 182:331–350

Chalker BE, Taylor DL (1975) Light enhanced calcification, and the role of oxidative phosphorylation in calcification of the coral *Acropora cervicornis*. Proc R Soc Lond (Biol) 190:323–331

Clode PL, Marshall AT (2003a) Skeletal microstructure of *Galaxea fascicularis* exert septa: a high-resolution SEM study. Biol Bull 204:146–154

Clode PL, Marshall AT (2003b) Calcium associated with a fibrillar organic matrix in the scleractinian coral *Galaxea fascicularis*. Protoplasma 220:153–161

Constantz BR (1986) Coral skeleton construction: a physiochemically dominated process. Palaios 1:152–157

Constantz BR (1989) Skeletal organization in Caribbean *Acropora* spp. (Lamarck). In: Crick RE (ed) Origin evolution and modern aspects of biomineralization in plants and animals. Plenum, New York, pp 175–199

Cuif JP, Dauphin Y (2005) The two-step mode of growth in the scleractinian coral skeletons from the micrometer to the overall scale. J Struct Biol 150:319–331

Cuif JP, Dauphin Y, Gautert P (1999) Compositional diversity of soluble mineralizing matrices in some recent coral skeletons compared to fine-scale growth structures of fibers: discussion of consequences for biomineralization and diagenesis. Int J Earth Sci 88:582–592

Furla P, Galgani I, Durand I, Allemand D (2000) Sources and mechanisms of inorganic carbon transport for coral calcification and photosynthesis. J Exp Biol 203:3445–3457

Gattuso JP, Allemand D, Frankignoulle M (1999) Photosynthesis and calcification at cellular, organismal and community levels in coral reefs: a review on interaction and control by carbonate chemistry. Am Zool 39:160–183

Gladfelter EH (1982) Skeletal development in *Acropora cervicornis*. I. Pattern of calcium carbonate accretion in the axial corallite. Coral Reefs 1:45–51

Gladfelter EH (1983) Skeletal development in *Acropora cervicornis*. II. Diel pattern of calcium carbonate accretion. Coral Reefs 2:91–100

Goreau TF (1959) The physiology of skeleton formation in corals. I. A method for measuring the rate of calcium deposition by corals under different conditions. Biol Bull 116:59–75

Hidaka M (1991) Deposition of fusiform crystals without apparent diurnal rhythm at the growing edge of septa of the coral *Galaxea fascicularis*. Coral Reefs 10:41–45

Hidaka M, Shirasaka S (1992) Mechanism of phototropism in young corallites of the coral *Galaxea fascicularis* (L.). J Exp Mar Biol Ecol 157:69–77

Howe SA, Marshall AT (2002) Temperature effects on calcification rate and skeletal deposition in the temperate coral *Plesiastrea versipora* (Lamark). J Exp Mar Biol Ecol 275:63–81

Isa Y (1986) An electron microscope study on the mineralization of the skeleton of the staghorn coral *Acropora hebes*. Mar Biol 93:91–101

Johnston IS (1980) The ultrastructure of skeletogenesis in hermatypic corals. Int Rev Cytol 67:171–214

Le Tissier MDÁA (1988) Diurnal patterns of skeleton formation in *Pocillopora damicornis* (Linnaeus). Coral Reefs 7:81–88

Le Tissier MDÁA (1990) The ultrastructure of the skeleton and skeletogenic tissues of the temperate coral *Caryophyllia smithii*. J Mar Biol Assoc UK 70:295–310

Le Tissier MDÁA (1991) The nature of the skeleton and skleletonic tissues in the Cnidaria. Hydrobiologia 216/217:397–402
Marin F, Smith M, Isa Y, Muyzer G, Westbroek P (1996) Skeletal matrices, muci, and the origin of invertebrate calcification. Proc Natl Acad Sci USA 93:1554–1559
Marshall AT, Wright OP (1993) Confocal laser scanning light microscopy of extra thecal epithelia of undecalcified scleractinian corals. Cell Tissue Res 272:533–543
Muscatine L (1990) The role of symbiotic algae in carbon and energy flux in reef corals. In: Dubinsky Z, et al (eds) Ecosystems of the world, vol 25. Elsevier, Amsterdam, pp 75–87
Ogilvie M (1896) Microscopic and systematic study of madreporarian types of corals. Philos Trans R Soc Lond Biol 187:85–345
Pearse VB, Muscatine L (1971) Role of symbiotic algae (zooxanthellae) in coral calcification. Biol Bull 141:350–363
Perrin C (2003) Compositional heterogeneity and microstructural diversity of coral skeleton: implications for taxonomy and control on early diagenesis. Coral Reefs 22:109–120
Reynaud-Vaganay S, Gattuso JP, Cuif JP, Jaubert J, Juillet-Leclerc A (1999) A novel culture technique for scleractinian corals: application to investigate changes in skeletal $\Delta^{18}O$ as a function of temperature. Mar Ecol Prog Ser 180:121–130
Rinkevich B, Loya Y (1984) Does light enhance calcification in hermatypic corals? Mar Biol 80:1–6
Rowley RJ, Mackinnon DT (1995) Use of the fluorescent marker Calcein in biomineralization studies of brachiopods and other marine organisms. Bull Inst Oceanogr (Monaco) SPEC 14:111–120
Shafir S, Van Rijn J, Rinkevich B (2001) Nubbing of coral colonies: a novel approach for the development of inland bloodstocks. Aquarium Sci Conserv 3:183–190
Shafir S, Van Rijn J, Rinkevich B (2003) The use of coral nubbins in coral reef ecotoxicology testing. Biomol Eng 20:401–406
Simkiss K, Wilbur KM (1989) Biomineralization, cell biology and mineral deposition. Academic Press, San Diego
Vago R, Gill E, Collingwood JC (1997) Laser measurements of coral growth. Nature 386:30–31
Wise SW (1972) Observations of fasciculi on developmental surfaces of scleractinian coral exoskeletons. Biomineralization 6:160–175
Wainwright SA (1963) Skeletal organization in the coral *Pocillopora damicorni*s. Q J Microsc Sci 104:169–183
Wright OP, Marshall AT (1991) Calcium transport across the isolated oral epithelium of scleractinian corals. Coral Reefs 10:37–40
Young SD (1971) Organic material from scleratinian coral skeletons. I. Variation in composition between several species. Comp Biochem Physiol 40B:113–120
Young SD (1973) Calcification and synthesis of skeletal organic material in the coral *Pocillopora damicornis*. Comp Biochem Physiol 44A:669–672